

# Integrating the optical Bloch equations with the `driveall` program: Further examples

R. M. Potvliege

Physics Department, Durham University, Durham DH1 3LE, UK

December 2023 and May 2024. Last revision: 27/06/2024

## Contents

<b>1</b>	<b>Introduction</b>	<b>1</b>
<b>2</b>	<b>A 4-state ladder system</b>	<b>2</b>
<b>3</b>	<b>Absorption on the D1 line of rubidium</b>	<b>3</b>
<b>4</b>	<b>Rabi oscillations</b>	<b>7</b>
	<b>References</b>	<b>8</b>

## 1 Introduction

Two examples illustrating the use of the `obe` and `mbe` modules are given in the article describing this library [1]. Three more examples, all focusing on the use of the `driveall` program for integrating the optical Bloch equations, are provided with the distribution. The first two demonstrate the use of the software for calculating steady-state properties (here absorption spectra). The third one concerns the calculation of time-dependent populations and coherences. These additional examples are briefly described in the present notes. The reader is invited to peruse the corresponding input files and the comments given therein for the technical details not discussed here, and the rest of the documentation for the options and functionalities not addressed by these programs. The Python programs used for plotting the figures shown in this document are also included in the distribution.

The explanations below assume that the codes are compiled and linked to the `lapack` and `blas` libraries by the command

```
gfortran -o CoOMBE ... -llapack -lblas
```

and that after compilation the program can be executed with the command `./CoOMBE < inputfile` where `inputfile` is the name of the file which the program should read from through the standard input stream. We provide a makefile for each example, which makes it possible to compile the program through a simple `make` command. However, these commands are system-dependent and may need to be adapted to the user's installation. Alternatively, the program can also be compiled and run through Podman, as explained in Appendix G of the article.

All the necessary information about the use of the `driveall` program can be found in Section 4 of the detailed documentation. We recommend that users unfamiliar with this software first read through Sections 4.1 and 4.2.1 and through the introductory paragraphs of Sections 4.2.2, 4.2.3 and 4.2.4 before studying the examples described below. In a few words, all the necessary information for running the code must be specified in certain input files, some of which are optional. Two are mandatory: a “`keyparams`” file, specifying key parameters as well as the name of the other mandatory file, the “`controlparams`” file. The latter and the optional files are meant to contain all the rest of the information required by the program for carrying out the desired computation.

## 2 A 4-state ladder system

This example shows how the present programs could be used for reproducing some of the calculations described in Ref. [2], specifically the calculations that yielded the results presented in Fig. 15 of that reference. This figure refers to a 4-state ladder system in which states 1 and 2 are coupled by a first field (the probe field), states 2 and 3 by a second field and states 3 and 4 by a third field. The problem at hand is to calculate the steady-state coherence  $\rho_{21}$  for a range of probe detunings, within the weak probe approximation and taking Doppler broadening into account.

As there are four states in the problem, the `general_settings` module must give a value of 4 to the variable `nst`, as done in the file `general_settings_4st.f90`. Compiling the `driveall` program would then be done by the command

```
gfortran -o CoOMBE general_settings_4st.f90
ldbl.f90 obe.f90 mbe.f90 driveall.f90 -llpack -lblas
```

The `keyparams` file for that example is `ladder.k.dat`: running the program is done by the command

```
./CoOMBE < ladder_k.dat
```

Doing so will produce a file called `ladder_rho21.dat` containing a table of values of  $\rho_{21}$  for probe detunings ranging from  $-30$  to  $30$  MHz (the first column

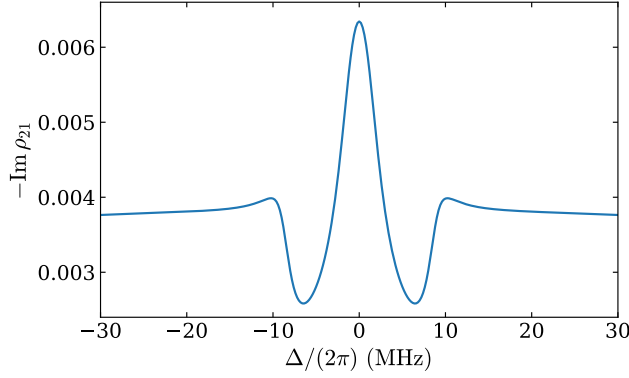


Figure 1: The imaginary part of the coherence  $\rho_{21}$  when calculated as described in Section 2.

of this table is the probe detuning, the second the real part of  $\rho_{21}$  and the third the imaginary part of  $\rho_{21}$ ). The name of this output file is specified in the `ladder.c.dat` file, which is itself specified in `ladder.k.dat` as being the `controlparams` file for this computation. The latter file, here, specifies settings which determine what should be calculate, how this should be calculated and what should be written out, as well all the necessary data: Rabi frequencies, decay rates, dephasing rates, detunings, the initial populations, and also the root-mean-squared velocity, wavelengths and propagation directions to be assumed in the Doppler averaging.

The resulting imaginary part of  $\rho_{21}$  is displayed in Fig. 1. These results are identical to those represented by the solid dark purple line in Fig. 15 of Ref. [2]. The results represented by the light purple line in that reference can be obtained by turning off the Doppler averaging, which would be done simply by changing `iDoppler = 1` by `iDoppler = 0` in `ladder.c.dat`. Changing `iweakprb = 1` by `iweakprb = 0` would remove the assumption of the weak probe approximation.

### 3 Absorption on the D1 line of rubidium

This second example illustrates the use of the software for the calculation of the absorption profile of an atomic vapour. The system considered is a pure  $^{85}\text{Rb}$  vapour addressed by a linearly polarized cw laser beam on resonance with the D1 line. The refractive index is calculated in three different ways: in the weak probe approximation, in the weak probe approximation with power broadening taken into account (as explained in the description of `obe_steadystate_onefld_powerbr` in Section 5.3.2 of the detailed documentation), and without assuming the weak probe approximation. For the sake of the example, the intensity of the field is taken to be above the saturation intensity of the transition ( $4.5 \text{ mW cm}^{-2}$  [3]), which causes significant power broaden-

ing and strong optical pumping. The hyperfine structure of the  $5^2S_{1/2}$  and  $5^2P_{1/2}$  states is taken into account, as is Doppler and collisional broadening. (The ground state and the  $5^2P_{1/2}$  state of  $^{85}\text{Rb}$  both have 12  $(F, m_F)$  hyperfine components with  $F$  values of either 2 or 3.) For simplicity, it is assumed that there is no magnetic or static electric field.

The data required for this calculation are the electric field amplitude of the laser field, the dipole matrix elements for all the allowed transitions between the 12  $(F, m_F)$  hyperfine components of the ground state and the 12  $(F', m'_F)$  components of the  $5^2P_{1/2}$  state, the spontaneous decay rate of the excited states and the corresponding branching ratios, the rates of dephasing originating from the collisions between atoms (self-broadening), the number density of the vapour, the r.m.s. thermal velocity of the atoms and the initial populations. These different quantities must be provided by the user as the necessary programs are not included in **obe** or **mbe**. The atomic data are chosen, in this example, to be identical to those used by the popular program Elecsus [5], which addresses similar calculations within the weak probe approximation.

The intensity of the applied field is taken to be  $10 \text{ mW cm}^{-2}$ . The corresponding electric field amplitude is easily calculated from the fact, mentioned in the detailed documentation, that a field of exactly  $1 \text{ mW cm}^{-2}$  intensity corresponds to an electric field amplitude  $\mathcal{E}$  of  $86.8021 \text{ V m}^{-1}$ . The electric field amplitude of the field considered in this example is larger by a factor  $\sqrt{10}$ : to six significant figures,  $\mathcal{E} = 274.492 \text{ V m}^{-1}$  here (there is no need to take the field amplitude to be complex in the present situation).

We take the field to be  $\pi$ -polarized in the  $z$ -direction. The corresponding matrix elements of the dipole operator take on the following form, for the D1 line of  $^{85}\text{Rb}$ :

$$\begin{aligned} \langle 5^2S_{1/2}(F, m_F) | D_z | 5^2P_{1/2}(F', m'_F) \rangle &= (-1)^{1-m_F} \langle 5^2S_{1/2} || er || 5^2P_{1/2} \rangle \\ &\times \sqrt{2(2F+1)(2F'+1)} \begin{pmatrix} F' & 1 & F \\ m'_F & 0 & -m_F \end{pmatrix} \begin{Bmatrix} 1/2 & 1/2 & 1 \\ F' & F & 5/2 \end{Bmatrix}, \quad (1) \end{aligned}$$

with  $\langle 5^2S_{1/2} || er || 5^2P_{1/2} \rangle = 2.537 \times 10^{-29} \text{ C m}$ . The value of this reduced dipole matrix element is obtained from the relation between this reduced dipole matrix element and the natural width of the  $5^2P_{1/2}$  state,  $\hbar\Gamma$ :

$$\langle 5^2S_{1/2} || er || 5^2P_{1/2} \rangle = \left( \frac{3\epsilon_0 \hbar \lambda^3 \Gamma}{8\pi^2} \right)^{1/2}, \quad (2)$$

with  $\lambda = 794.979 \text{ nm}$  and  $\Gamma = 2\pi \times 5.746 \text{ MHz}$  [4, 5].

While each of the  $(F', m'_F)$  hyperfine component of the  $5^2P_{1/2}$  state has a same total rate of spontaneous decay  $\Gamma$ , the program requires the rates of decay to specific hyperfine components of the ground state (these rates are the  $\Gamma_{ij}$ 's defined in the detailed documentation, here with the index  $j$  referring to the different  $5^2P_{1/2}(F', m'_F)$  states and the index  $i$  to the different  $5^2S_{1/2}(F, m_F)$  states). Each of these decay rates can be obtained by multiplying  $\Gamma$  by the

respective branching ratio,

$$b[5^2P_{1/2}(F', m'_F) \rightarrow 5^2S_{1/2}(F, m_F)] = \frac{2(2F+1)(2F'+1)}{\sum_{q=-1,0,1}} \left[ \begin{pmatrix} F' & 1 & F \\ m'_F & q & -m_F \end{pmatrix} \begin{Bmatrix} 1/2 & 1/2 & 1 \\ F' & F & 5/2 \end{Bmatrix} \right]^2. \quad (3)$$

The program also requires the value of  $\delta\omega^{(i)}$  for each of the states considered, unless this quantity is zero. As is explained in the detailed documentation,  $\hbar\delta\omega^{(i)}$  is the energy of state  $i$  measured with respect to a user-defined reference level  $\hbar\omega_{\text{ref}}$ . The choice of the latter is arbitrary. One possibility is to refer the hyperfine states to the centroid of their respective doublet, in which case  $\delta\omega^{(i)}/(2\pi)$  would be 1264.889 MHz for the  $5^2S_{1/2}(F=3)$  states,  $-1770.844$  MHz for the  $5^2S_{1/2}(F=2)$  states, 150.659 MHz for the  $5^2P_{1/2}(F=3)$  states and  $-210.923$  MHz for the  $5^2P_{1/2}(F=2)$  states [3]. The frequency detuning would then be measured with respect to the difference between the two centroids, i.e., 377.107 385 690 THz [3]. Another choice, which is the one adopted in this example for consistency with the Elecsus program [5], is to measure the frequency detuning with respect to the linecentre frequency averaged over the two natural isotopes of rubidium, 377.107 407 299 THz [5]. This choice can be implemented, in the present calculation, by defining the  $\delta\omega^{(i)}$ 's with respect to the ground state hyperfine centroid for the  $5^2S_{1/2}$  states, as above, and with respect to the point 377.107 407 299 THz above the ground state centroid for the  $5^2P_{1/2}$  states. Within this choice,  $\delta\omega^{(i)}/(2\pi) = 129.050$  MHz for the  $5^2P_{1/2}(F=3)$  states and  $-232.532$  MHz for the  $5^2P_{1/2}(F=2)$  states,

The temperature of the vapour is chosen to be 80 °C in this example. The corresponding rms atomic velocity  $u$  is 262.983 m s<sup>-1</sup> ( $u = \sqrt{2k_B T/M}$  with, here,  $T = 353.15$  K and  $M = 84.9118$  u). The number density,  $N_d$ , is  $1.54882 \times 10^{18}$  m<sup>-3</sup> at that temperature, as calculated by standard methods [3, 5]. This number density is sufficiently high that collisional broadening (self-broadening) needs to be taken into account for precise calculations. In the weak probe limit, collisional broadening contributes a decay rate  $\beta N_d$  additional to the spontaneous decay rate  $\Gamma$ , where [6, 7]

$$\beta = \frac{\lambda^3 \Gamma}{4\pi^2}. \quad (4)$$

The effect is best treated as a dephasing process in calculations beyond the weak probe approximation. As such, it can be taken into account through additional dephasing rates, namely

$$\gamma_{ij} = \frac{\lambda^3 N_d}{8\pi^2} \Gamma_{ij}. \quad (5)$$

Finally, the atoms can be assumed to have an equal probability to be initially in any of the 12 hyperfine component of the ground state and a zero probability to be in an excited state. The corresponding initial populations are 1/12 for the ground state populations and 0 for the  $5^2P_{1/2}$  populations.

In view of the volume of the corresponding data, passing the required dipole matrix elements, decay rates, additional dephasing rates and initial populations to the program is best done through the `defaultdata` file, as this file can be written once and for all and does not need to be changed when varying, e.g., the temperature of the vapour or the method of calculation. In this example, this `defaultdata` file is the file called `Rb85D1.d.dat`. The name of this file and the name of the `controlparams` file (`Rb85D1.c.dat`) are specified in the `keyparams` file (here `Rb85D1.k.dat`). Running the code for this example can thus be done through the command

```
CoOMBE < Rb85D1_k.dat
```

once the code has been compiled. Since there are 24 states in this example, the `general_settings` module must give a value of 24 to the variable `nst`, as done in the file `general_settings_24st.f90`. Compiling the `driveall` program could then be done by the command

```
gfortran -o CoOMBE general_settings_24st.f90
        ldbl.f90 obe.f90 mbe.f90 driveall.f90 -llpack -lblas
```

The `controlparams` file `Rb85D1.c.dat` contains all the rest of the necessary information, including the wavelength and electric field amplitude of the applied field, the atomic density, the rms thermal velocity of the atoms and the name of the output file. How to select the method of calculation of the complex refractive index is also explained in `Rb85D1.c.dat`. Given that the computation needs to be repeated for a number of detunings, it is done, for efficiency, using the method outlined in appendix B of the article. The calculations beyond the weak field approximation are prone to be affected to some extent by numerical instabilities, within this method, and for that reason need to be done in double precision arithmetic. At the probe intensity considered in this example, these instabilities may manifest by minor and unimportant differences between results obtained with different compilers. These difference reduce further at higher intensities.

The values of the absorption coefficient produced by the program for the three calculation methods considered are displayed in Fig. 2. The solid blue curve, showing the results obtained within the weak probe approximation, are identical to the results produced by the Elecsus program for the same choice of parameters. Including power broadening within the weak probe approximation reduces the absorption coefficient at resonance, without noticeably broadening the two peaks as the width of the peaks is dominated by the much larger Doppler broadening). However, doing the calculation beyond the weak probe approximation gives a different picture altogether, as shown by the green dotted curve: optical pumping tends to redistribute the population to those hyperfine components of the ground state that are least strongly coupled to the  $5^2P_{1/2}$  state, which at most detunings leads to a considerable reduction of the absorption coefficient compared to the values obtained within the weak probe approximation.

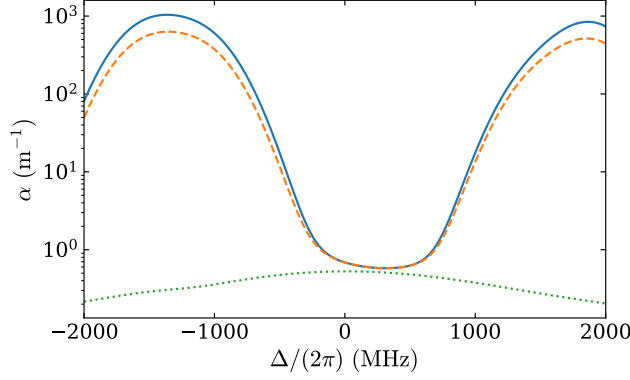


Figure 2: The variation of the absorption coefficient with the detuning across the D1 line of  $^{85}\text{Rb}$ , for a linearly polarized cw field of  $10 \text{ mW cm}^{-2}$  intensity, in the example discussed in Section 3. The zero of the detuning axis corresponds to a field of  $377.107\,407\,299 \text{ THz}$  frequency. Solid blue curve: results obtained in the weak probe approximation without allowance for power broadening. Dashed orange curve: results obtained in the weak probe approximation with power broadening taken into account. Dotted green curve: results obtained when the weak probe approximation is not made and hyperfine pumping is taken into account.

## 4 Rabi oscillations

This example addresses the case where the density matrix needs to be calculated as a function of time. For simplicity, the system considered here contains only two states. It is the same system as that considered in Section 3, though, but now neglecting Doppler broadening and the hyperfine structure of the states: State 1 is the ground state of an atom of  $^{85}\text{Rb}$ , state 2 is the  $5^2\text{P}_{1/2}$  state, and the dipole moment has the value expected for the coupling of these two fine structure states by a linearly polarized field:

$$\langle 5^2\text{S}_{1/2} | D_z | 5^2\text{P}_{1/2} \rangle = \langle 5^2\text{S}_{1/2} || er || 5^2\text{P}_{1/2} \rangle / \sqrt{3}. \quad (6)$$

We take  $\langle 5^2\text{S}_{1/2} || er || 5^2\text{P}_{1/2} \rangle = 2.537 \times 10^{-29} \text{ C m}$  and  $\Gamma = 2\pi \times 5.746 \text{ MHz}$ , as in Section 3. However, in the present example we take the applied field to be a pulse with a Gaussian intensity profile of  $0.8 \text{ ns}$  duration (fwhm) and  $1 \text{ kW cm}^{-2}$  peak intensity centered at time  $t = 0$ . The system is initially in the ground state. The optical Bloch equations are integrated between  $-2 \text{ ns}$  and  $2 \text{ ns}$  using the `dop853` integrator. The program produces a table of values of the ground state population  $\rho_{11}(t)$  and of the coherence  $\rho_{12}(t)$  for a number of intermediate times. The weak probe approximation is not assumed.

Since there are two states, the `general_settings` module must give a value of 2 to the variable `nst`, as done in the file `general_settings_2st.f90`. Compiling the `driveall` program would then be done by the command

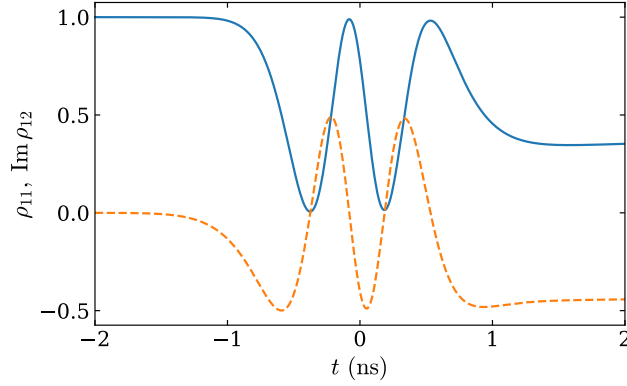


Figure 3: The variation of  $\rho_{11}(t)$  (solid blue curve) and of the imaginary part of  $\rho_{12}(t)$  (dashed orange curve) in 2-state system driven by a Gaussian pulse, as obtained by integrating the optical Bloch equations as described in Section 4.

```
gfortran -o CoOMBE general_settings_2st.f90
        ldbl.f90 obe.f90 mbe.f90 driveall.f90 -llpack -lblas
```

The `keyparams` file for that example is `timedep_k.dat`: running the program is done by the command

```
CoOMBE < timedep_k.dat
```

Doing so will produce the files `timedep_rho11.dat` and `timedep_rho21.dat` containing the results. The names of these two output files and the rest of the necessary information, including the parameters defining the applied pulse, is specified in the `timedep_c.dat` file. The latter is itself specified in `timedep_k.dat` as being the `controlparams` file for this computation. The results are shown in Fig. 3.

## References

- [1] R. M. Potvliege and S. A. Wrathmall, CoOMBE: A suite of open-source programs for the integration of the optical Bloch equations and Maxwell-Bloch equations, submitted for publication (2024).
- [2] L. Downes, Simple Python tools for modelling few-level atom-light interactions, *J. Phys. B: At. Mol. Opt. Phys.* **56**, 223991 (2023).
- [3] D. A. Steck, Rubidium 85 D Line Data, available online at <http://steck.us/alkalidata> (revision 2.3.2, 10 December 2023).



- [4] U. Volz and H. Schmoranzer, Precision lifetime measurements on alkali atoms and on helium by beam-gas-laser spectroscopy, *Phys. Scr.* **T65**, 48 (1996).
- [5] M. A. Zentile, J. Keaveney, L. Weller, D. J. Whitting, C. S. Adams and I. G. Hughes, ElecSus: A program to calculate the electric susceptibility of an atomic ensemble, *Comput. Phys. Comm.* **189**, 162 (2015).
- [6] E. L. Lewis, Collisional relaxation of atomic excited states, line broadening and interatomic interactions, *Phys. Rep.* **58**, 1 (1980).
- [7] L. Weller, R. J. Bettles, P. Siddons, C. S. Adams and I. G. Hughes, Absolute absorption on the rubidium  $D_1$  line including resonant dipole-dipole interactions, *J. Phys. B.: At. Mol. Opt. Phys.* **44**, 195006 (2011).
- [8] T. P. Ogden, K. A. Whittaker, J. Keaveney, S. A. Wrathmall, C. S. Adams and R. M. Potvliege, Quasisimultons in thermal atomic vapors, *Phys. Rev. Lett.* **123**, 243604 (2019).
- [9] S. L. McCall and E. L. Hahn, Self-induced transparency by pulsed coherent light, *Phys. Rev. Lett.* **18**, 908 (1967).